Article

Dual Function of the Hydration Layer around an Antifreeze Protein Revealed by Atomistic Molecular Dynamics Simulations

David R. Nutt, and Jeremy C. Smith

J. Am. Chem. Soc., **2008**, 130 (39), 13066-13073 • DOI: 10.1021/ja8034027 • Publication Date (Web): 06 September 2008

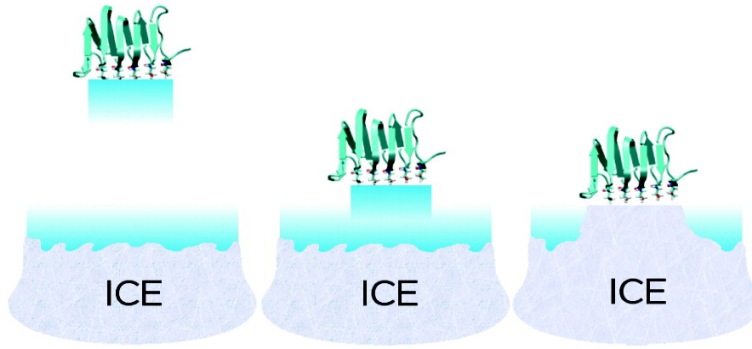

J|A|C|S
ARTICLES

Published on Web 09/06/2008

Dual Function of the Hydration Layer around an Antifreeze Protein Revealed by Atomistic Molecular Dynamics Simulations

David R. Nutt*,†,‡ and Jeremy C. Smith‡,§

Computational Molecular Biophysics, IWR, Im Neuenheimer Feld 368, University of Heidelberg, 69120 Heidelberg, Germany, and Center for Molecular Biophysics, Oak Ridge National Laboratory/University of Tennessee, P.O. Box 2008, 1 Bethel Valley Road, Oak Ridge, Tennessee 37831

Received May 7, 2008; E-mail: d.nutt@reading.ac.uk

Abstract: Atomistic molecular dynamics simulations are used to investigate the mechanism by which the antifreeze protein from the spruce budworm, *Choristoneura fumiferana*, binds to ice. Comparison of structural and dynamic properties of the water around the three faces of the triangular prism-shaped protein in aqueous solution reveals that at low temperature the water structure is ordered and the dynamics slowed down around the ice-binding face of the protein, with a disordering effect observed around the other two faces. These results suggest a dual role for the solvation water around the protein. The preconfigured solvation shell around the ice-binding face is involved in the initial recognition and binding of the antifreeze protein to ice by lowering the barrier for binding and consolidation of the protein:ice interaction surface. Thus, the antifreeze protein can bind to the molecularly rough ice surface by becoming actively involved in the formation of its own binding site. Also, the disruption of water structure around the rest of the protein helps prevent the adsorbed protein becoming covered by further ice growth.

1. Introduction

Since the first report in 1969 of antifreeze proteins (AFPs)[1−3] occurring in Antarctic fish,[4] AFPs have been identified in a wide range of organisms, including moths,[5] snow fleas,[6] plants,[7] and bacteria.[8] Their unique properties offer the potential of a wide range of applications, from increasing the cold tolerance of plants through genetic engineering[9] to improved cryopreservation techniques,[10] as well as in the food industry.[11]

At the molecular level, AFPs are believed to function by an adsorption-inhibition mechanism.[1] In a first step, the proteins recognize and bind quasi-irreversibly to the ice surface.[12] Further ice growth is then possible only in the regions between adsorbed proteins, where the ice is forced to grow with a curved interface. The interfacial curvature leads to a reduction in the local freezing temperature due to the Kelvin effect, while leaving the melting temperature unchanged. The magnitude of the freezing point depression can be used as a measure of the antifreeze activity of a particular protein. If the solution is cooled below the reduced freezing point, the AFPs are overgrown and incorporated into the ice crystal.[12]

Ice recognition is typically performed by one specific face of the protein (the ice-binding face), which tends to be topologically flat and relatively hydrophobic.[13] Intrinsic surface complementarity between ice and the AFP appears to be a prerequisite for antifreeze activity.[14] This is exemplified by the case of the hyperactive AFPs from the insects *Tenebrio molitor* and *Choristoneura fumiferana*, in which the ice-binding is performed by a two-dimensional array of threonine residues on a flat β-sheet region.[5,15] Extension of the ice-binding surface by protein engineering was found to increase the antifreeze activity.[16] Confirmation that the array of threonine residues is the ice-binding surface was provided by mutation studies[5] in which it was shown that replacing threonine residues in the two-dimensional array with leucine reduced the antifreeze activity

† Current address: Department of Chemistry, The University of Reading, PO BOX 224, Whiteknights, Reading RG6 6AD, UK.
‡ University of Heidelberg.
§ Oak Ridge National Laboratory/University of Tennessee.

(1) Yeh, Y.; Feeney, R. E. *Chem. Rev.* **1996**, *96*, 601–618.
(2) Duman, J. G. *Annu. Rev. Physiol.* **2001**, *63*, 327–357.
(3) Fletcher, G. L.; Hew, C. H.; Davies, P. L. *Annu. Rev. Physiol.* **2001**, *63*, 359–390.
(4) DeVries, A. L.; Wohlschlag, D. E. *Science* **1969**, *163*, 1073–1075.
(5) Graether, S. P.; Kuiper, M. J.; Gagné, S. M.; Walker, V. K.; Jia, Z.; Sykes, B. D.; Davies, P. L. *Nature* **2000**, *406*, 325–328.
(6) Graham, L. A.; Davies, P. L. *Science* **2005**, *310*, 461.
(7) Sidebottom, C.; Buckley, S.; Pudney, P.; Twigg, S.; Jarman, C.; Holt, C.; Telford, J.; McArthur, A.; Worrall, D.; Hubbard, R.; Lillford, P. *Nature* **2000**, *406*, 256.
(8) Gilbert, J. A.; Hill, P. J.; Dodd, C. E.; Laybourn-Parry, J. *Microbiology* **2004**, *150*, 171–180.
(9) Fan, Y.; Liu, B.; Wang, H.; Wang, S.; Wang, J. *Plant Cell Rep.* **2002**, *21*, 296–301.
(10) Rubinsky, B.; Arav, A.; DeVries, A. L. *Cryobiology* **1992**, *29*, 69–79.
(11) Griffith, M.; Ewart, K. V. *Biotechnol. Adv.* **1995**, *13*, 375–402.
(12) Pertaya, N.; Marshall, C. B.; DiPrinzio, C. L.; Wilen, L.; Thomson, E. S.; Wettlaufer, J. S.; Davies, P. L.; Braslavsky, I. *Biophys. J.* **2007**, *92*, 3663–3673.
(13) Davies, P. L.; Baardsnes, J.; Kuiper, M. J.; Walker, V. K. *Philos. Trans. R. Soc. London, Ser. B* **2002**, *357*, 927–935.
(14) Leinala, E. K.; Davies, P. L.; Jia, Z. *Structure* **2002**, *10*, 619–627.
(15) Liou, Y.-C.; Tocilj, A.; Davies, P. L.; Jia, Z. *Nature* **2000**, *406*, 322–324.
(16) Marshall, C. B.; Daley, M. E.; Sykes, B. D.; Davies, P. L. *Biochemistry* **2004**, *43*, 11637–11646.

 10.1021/ja8034027 CCC: $40.75

by 80−90%, whereas mutation of threonines elsewhere in the protein produced little or no effect.

In contrast to other inorganic surfaces to which proteins can bind, such as calcium oxalate in human kidney stones,[17] an ice surface is not well ordered at the molecular level, and computer simulations have shown that the interfacial region between bulk ice and bulk water is around 10−15 Å thick.[18,19] Although the ice-binding model based on surface complementarity is now generally accepted,[14] it remains unclear how AFPs are able to recognize a surface which is intrinsically disordered.

Experimental studies on the growth of ice in the presence of AFP from winter flounder showed that the AFPs can stabilize ice planes which are not normally expressed in macroscopic crystals, thus providing a first indication that the binding of AFP occurs in conjunction with the local growth of ice.[20] However, the proposed "zipper mechanism" requires the AFP to be partially bound to the ice before it can shape the ice surface, and therefore does not describe the initial steps of the recognition process. Subsequent simulations of a small AFP at the ice−water interface led to the suggestion that the interfacial layer between the bulk phases may play an important role in the ice-recognition process.[21] More recent simulations on type I and type III antifreeze proteins have also indicated that the protein−water interactions at different faces of the protein contribute to the adsorption free energy, along with the binding surface area and the side-chain conformations.[22,23] In addition, recent simulations have provided insight into the molecular basis of the freezing point depression and ice-growth inhibition mechanism of a mutant of the winter flounder AFP.[24]

It is well-known that protein hydration water exhibits properties very different to bulk water and can play an important role in controlling protein function.[25] The present molecular dynamics simulation analysis on the antifreeze protein from the spruce budworm, *Choristoneura fumiferana*, suggests that the inverse can also be true—that the protein can control the properties of the hydration water in order to optimize its activity. It is shown that, in aqueous solution in the absence of ice, the ice-binding face of the AFP preorganizes its solvation water into an ordered, quasi ice-like structure. This suggests that AFP binding to ice is mediated by the preordered AFP surface water. The existence of the ordered hydration water may overcome the potential difficulty arising from the ill-defined nature of ice surfaces, by promoting growth of ice between the ordered hydration water and the ice surface, thus "bringing the ice surface to the protein", rather than the protein itself having to directly bind to the ice. Furthermore, a second functional role also appears to be fulfilled by the solvation water: disruption of the water structure around the non-ice-binding parts of the protein is observed, providing a mechanism to help prevent the adsorbed protein being overgrown by a growing ice surface.

2. Methods

Simulations of AFPs at an ice−water interface are computationally expensive. Furthermore, the information required, on the mechanism by which the AFP perturbs water properties, can be obtained from the simulation of the protein in a uniform aqueous solution. Consequently, the results presented here are of a single AFP molecule in a box of liquid water, replicated with periodic boundary conditions.

Classical molecular dynamics (MD) was performed using the CHARMM program[26] together with the CHARMM22 parameter set.[27] Simulations were performed at two temperatures, 250 and 300 K, corresponding to temperatures above and below the freezing point of water (but above the glass transition temperature) in the microcanonical (NVE) ensemble, with a 1 fs time step. The SHAKE algorithm was used to constrain all bonds to hydrogen[28] and the water molecules were treated as rigid. Nonbonded interactions were gradually brought to zero using a shift function for the electrostatics and a switch function for the van der Waals interactions between 10 and 12 Å, consistent with the methodology used in the development of most empirical water models used in biomolecular simulations. The NVE ensemble was used to avoid the velocity tampering effects introduced by the various thermostats and barostats used in the canonical (NVT) and isothermal−isobaric (NpT) ensembles.[29]

Since isolated AFPs in vitro are active over a small temperature range around 0 °C, special care must be taken in the choice of the computational representation of the water. Given that the properties of water are central to the function of AFPs, it is essential that they are reproduced as accurately as possible, within the limits of available computational resources. The TIP5P water model[30] is therefore an appropriate choice for the present simulations, since it provides a better representation of water under the chosen simulation conditions than the CHARMM default, the TIP3P model,[27,31] for which the melting temperature has recently been determined to be around 146 K.[32] Similar concerns have been raised in other recent simulations.[23,24] Since the CHARMM22 force field was originally parametrized for use with a modified TIP3P water model,[31] its substitution with a different model could potentially lead to an imbalance between water−water and water−protein interactions.[27] However, we have recently shown that this is not the case and that the overall description of peptide solvation using TIP3P and TIP5P water is similar.[33] Nevertheless, any force-field description may possess unquantified systematic errors. In the present case, the subtle effect of the small thermal hysteresis of even hyperactive AFPs (a few degrees) is unlikely to be accurately reproduced with current force fields. For this reason, simulations were performed at temperatures above and below the experimental freezing point. At the lower temperature, it is important to note that the water is only supercooled, and not frozen (it is typically notoriously difficult to observe freezing in computer simulations),[34] nor glassy (T_g for TIP5P water has been calculated to be at 215

(17) Wang, L.; Qiu, S. R.; Zachowicz, W.; Guan, X.; DeYoreo, J. J.; Nancollas, G. G.; Hoyer, J. R. *Langmuir* **2006**, *22*, 7279–7285.
(18) Mantz, Y. A.; Geiger, F. M.; Molina, L. T.; Molina, M. J.; Trout, B. L. *J. Chem. Phys.* **2000**, *113*, 10733–10743.
(19) Hayward, J. A.; Haymet, A. D. J. *J. Chem. Phys.* **2001**, *114*, 3713–3726.
(20) Houston, M. E., Jr.; Chao, H.; Hodges, R. S.; Sykes, B. D.; Kay, C. M.; Sönnichsen, F. D.; Loewen, M. C.; Davies, P. L. *J. Biol. Chem.* **1998**, *273*, 11714–11718.
(21) Madura, J. D.; Baran, K.; Wierzbicki, A. *J. Mol. Recognit.* **2000**, *13*, 101–113.
(22) Wierzbicki, A.; Dalal, P.; Cheatham, T. E.; Knickelbein, J. E.; Haymet, A. D. J.; Madura, J. D. *Biophys. J.* **2007**, *93*, 1442–1451.
(23) Smolin, N.; Daggett, V. *J. Phys. Chem. B* **2008**, *112*, 6193–6202.
(24) Nada, H.; Furukawa, Y. *J. Phys. Chem. B* **2008**, *112*, 7111–7119.
(25) Frauenfelder, H.; Fenimore, P. W.; McMahon, B. H. *Biophys. Chem.* **2002**, *98*, 35–48.
(26) Brooks, B. R.; Bruccoleri, R. E.; Olafson, B. D.; States, D. J.; Swaminathan, S.; Karplus, M. *J. Comput. Chem.* **1983**, *4*, 187–217.
(27) MacKerell, A. D.; Jr.; et al. *J. Phys. Chem. B* **1998**, *102*, 3586–3616.
(28) Ryckaert, J. P.; Ciccotti, G.; Berendsen, H. J. C. *J. Comput. Phys.* **1977**, *23*, 327–341.
(29) Laage, D.; Hynes, J. T. *Chem. Phys. Lett.* **2006**, *433*, 80–85.
(30) Mahoney, M. W.; Jorgensen, W. L. *J. Chem. Phys.* **2000**, *112*, 8910–8922.
(31) Jorgensen, W. L.; Chandrasekhar, J.; Madura, J. D.; Impey, R. W.; Klein, M. L. *J. Chem. Phys.* **1983**, *79*, 926–935.
(32) Vega, C.; Sanz, E.; Abascal, J. L. F. *J. Chem. Phys.* **2005**, *122*, 114507.
(33) Nutt, D. R.; Smith, J. C. *J. Chem. Theory Comput.* **2007**, *3*, 1550–1560.
(34) Matsumoto, M.; Saito, S.; Ohmine, I. *Nature* **2002**, *416*, 409.

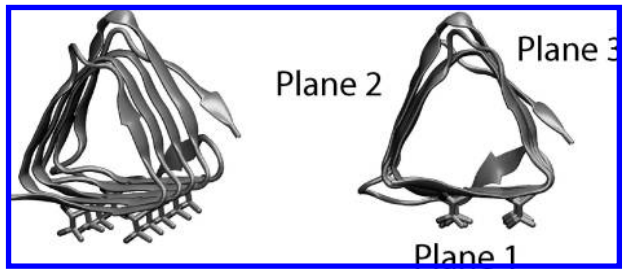

Figure 1. Two views of the antifreeze protein from *Choristoneura fumiferana*. The ice-binding threonines are shown and the protein planes are labeled.

K,[35] compared with the experimental values of between 136 and 160 K),[36,37] and that the Stokes−Einstein relation continues to hold.[38]

The 2.3 Å resolution X-ray crystal structure of the AFP from the spruce budworm *Choristoneura fumiferana* (CfAFP) was taken from the PDB file 1L0S[14] and is shown in Figure 1. Missing residues and hydrogen atoms were built into the structure, the iodated tyrosine Y26 required for the structure determination was reverted to a standard tyrosine, and the structure was energy minimized for 100 steps with the adopted basis Newton−Raphson (ABNR) algorithm. The protein was solvated in a cubic water box of TIP5P water of side 70 Å, which had previously been equilibrated at the required temperature. Any water molecules with an oxygen atom within 2.8 Å of a protein atom were deleted.

The protein was initially fixed and the water molecules energy minimized for 100 steps with the steepest descent algorithm to remove bad contacts. The system was then equilibrated at the required temperature for 400 ps. For the first 100 ps the protein was held fixed before subsequently being released. Velocity rescaling was performed when required during the initial 300 ps, after which time the energy was found to be stable. Following the equilibration, trajectories of 8 and 4 ns were calculated at 250 and 300 K, respectively, with coordinate sets saved every 100 fs.

The structural and dynamic properties of the solvation water were determined around the different faces of the protein. Exploiting the regular triangular prism shape of CfAFP (see Figure 1), the trajectories were reoriented such that each protein plane was aligned in turn to the *xy* -plane, with the protein center of mass at negative *z*. In the Results, Plane 1 refers to the ice-binding plane, with the other planes designated as Planes 2 and 3. The analysis region was defined geometrically by $-15 \le x \le 15$, $-8 \le y \le 8$ and $z > 0$ (distances in Å). For every water molecule in the analysis region, the distance to the closest non-hydrogen protein atom was determined, binned with a resolution of 0.1 Å, and subsequently normalized to form a density distribution function, $g(r)$. The minima in the density distribution function were then used to define solvation shells (SS): SS1, $0 < R < 3.1$; SS2, $3.1 \le R < 5.4$; SS3, $5.4 \le R < 8.5$; and SS4, $8.5 \le R$, where R is the distance (in Å) between a water oxygen atom and the nearest protein heavy atom.

3. Results

3.1. Water Is More Structured around the Ice-Binding Face. The structural properties of solvation water are quantified through the solvent density distribution function (analogous to the radial distribution function for pure liquids) and the local arrangement of molecules. The density distribution function, $g(r)$, reveals the thickness and relative density of the solvation shells, providing information about layering.

The local three-dimensional arrangement of molecules can be probed by the angles between hydrogen-bonded water molecules and the local tetrahedrality. The water−water angular distribution function, $P(\theta)$, is a pair property and describes the hypothetical hydrogen-bonding angle between neighboring water molecules.[39,40] The angle is defined as the smallest of the four H−O···O angles between two water molecules separated by a maximum distance of 4 Å. The geometry of TIP5P water means that this angle can take values between 0° and 128°. Although $P(\theta)$ is strictly a pair property, the distribution obtained has been found to be highly sensitive to the nature of the local environment (e.g., hydrophobic vs hydrophilic) and $P(\theta)$ has therefore been used to investigate the solvation of type I and type III AFPs.[23,40−42]

The local tetrahedrality is a many-body property and can be defined[43] by

$$S_g = 1 - \frac{3}{32}\sum_{j<k}^{6}\left(\cos\theta_{jik} + \frac{1}{3}\right)^2 \qquad (1)$$

where the sum is over all angles θ_{jik} formed around a reference molecule i by its four nearest potentially hydrogen-bonding neighbors, although no account is taken of whether the neighbors are actually hydrogen bonded to molecule i. A larger value of S_g indicates a greater local tetrahedrality. In the case of water molecules close to the protein, nearest neighbors are taken to include potential hydrogen-bonding moieties of the protein, such as threonine hydroxyl groups or the amide bonds of the protein backbone. Close to the protein surface, there will undoubtedly be water molecules in a constricted environment which cannot form tetrahedral structures, and this is reflected in the low values in S_g at smaller values of R.

Results for $g(r)$ and S_g are shown in Figure 2 and a plot of $P(\theta)$ is shown in Figure 3. At both temperatures, the solvent density, $g(r)$, around the non-ice-binding planes (2 and 3) is similar, with the large first peak at ≈2.8 Å suggesting a hydrophilic surface and tightly bound water molecules, due in part to the presence of charged and polar residues. In contrast, around the ice-binding plane (Plane 1), the first peak is smaller. As the scale is the same for all distributions, this indicates that there are fewer water molecules in the first solvation shell around the ice-binding face than near to the non-ice-binding faces. This illustrates a clear difference between the protein surfaces and suggests an analogy with ice and liquid water, where the former has fewer nearest neighbors than the latter. The size of the second peak increases slightly for Planes 2 and 3 on going from 300 to 250 K, but this increase is much more significant for Plane 1, for which the peaks in $g(r)$ corresponding to the first and second solvation shells have approximately the same magnitude at 250 K. This indicates that, at the lower temperature, the water around the ice-binding face is more structured than around the other two faces.

The plot of S_g (Figure 2, bottom) reveals very little difference between the three planes at 300 K. At 250 K, however, the tetrahedrality of the first two solvation shells (up to 6 Å from

(35) Brovchenko, I.; Geiger, A.; Oleinikova, A. *J. Chem. Phys.* **2005**, *123*, 044515.
(36) Velikov, V.; Borick, S.; Angell, C. A. *Science* **2001**, *294*, 2335–2338.
(37) Angell, C. A. *Annu. Rev. Phys. Chem.* **2004**, *55*, 559–583.
(38) Kumar, P.; Buldyrev, S. V.; Becker, S. R.; Poole, P. H.; Starr, F. W.; Stanlet, H. E. *Proc. Natl. Acad. Sci.* **2007**, *104*, 9575–9579.
(39) Henn, A. R.; Kauzmannm, W. *J. Phys. Chem.* **1989**, *93*, 3770–3783.
(40) Gallagher, K. R.; Sharp, K. A. *Biophys. Chem.* **2003**, *105*, 195–209.
(41) Yang, C.; Sharp, K. A. *Biophys. Chem.* **2004**, *109*, 137–148.
(42) Yang, C.; Sharp, K. A. *Proteins: Struct., Funct., Bioinformatics* **2005**, *59*, 266–274.
(43) Chau, P.-L.; Hardwick, A. J. *Mol. Phys.* **1998**, *93*, 511.

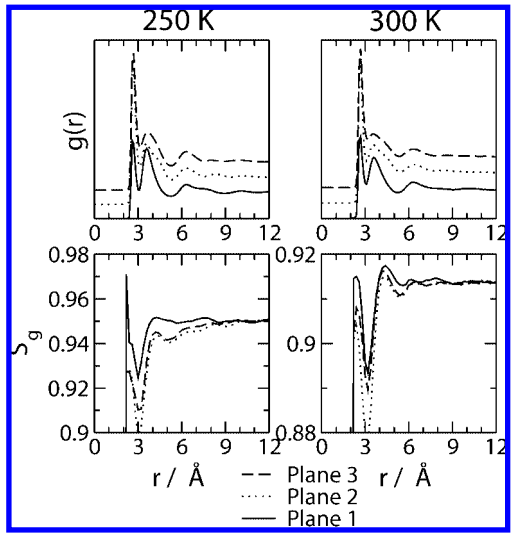

Figure 2. Structural properties of solvation water around the different planes of CfAFP at 250 (left) and 300 K (right). (Top) solvent density distribution ($g(r)$), and (bottom) local tetrahedrality (S_g) as a function of the distance to the nearest protein heavy atom. Plane 1, solid; Plane 2, dotted; Plane 3, dashed. The ordering is enhanced around the ice-binding face (Plane 1), especially at the lower temperature. The density distribution functions for Planes 2 and 3 have been displaced vertically for clarity.

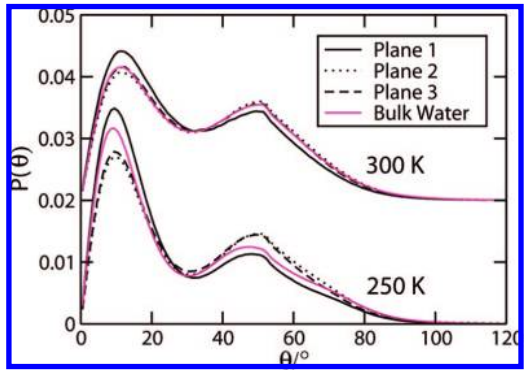

Figure 3. Water−water angle probability distributions for water around the different planes of CfAFP at 250 K (bottom) and 300 K (top). Plane 1, solid; Plane 2, dotted; Plane 3, dashed. The low-angle population is increased around the ice-binding face and reduced around Planes 2 and 3 at 250 K. Only water around the ice-binding face is affected at the higher temperature.

the protein) is significantly higher around the ice-binding plane than around Planes 2 and 3, indicating increased three-dimensional ordering of the water molecules. The large peak at low r is consistent with the presence of water molecules between the two rows of threonine residues, as observed experimentally in the crystal structure of the structurally similar TmAFP.[15] The lower tetrahedrality around Planes 2 and 3 indicates that the water structure is disrupted in these regions, providing a mechanism against the protein being engulfed by ice once binding has occurred.

The water−water angle distributions, $P(\theta)$, all exhibit two peaks, at $\theta \approx 10°$ and $\theta \approx 48°$, associated with more and less tetrahedral water, respectively (Figure 3). Previous studies on the detailed solvation of proteins and model compounds have indicated that the heights of the low- and high-θ peaks are increased in the region of hydrophobic and hydrophilic groups, respectively.[40,42] Strictly, it is not the peak height, but the area of the two peaks (separated at the minimum at $\theta \approx 30°$) which is important, but given that the minimum is in approximately the same position for all distributions, the heights of the peaks can be compared directly.

At 300 K, there are negligible differences in $P(\theta)$ between the protein solvation shells and bulk water around faces 2 and 3. Around the ice-binding face, there is a very slight increase in the low-θ population and a corresponding decrease at high-θ for the first solvation shell, indicating a slightly higher hydrophobic interaction around the ice-binding threonines. At 250 K, however, the differences become more significant. Around the ice-binding face, the low-θ population is significantly increased, with the opposite observed for Planes 2 and 3. The properties around Plane 1 are in agreement with previous studies of the solvation shell of ice-binding faces of different AFPs,[23,40−42] in which hydrophobic solvation was observed around the ice-binding face, even in the presence of hydrogen-bonding groups. In the case of CfAFP, the threonine residues appear to provide a suitable balance of hydrophobicity and hydrophilicity for effective ice binding. The increase in the population of less tetrahedral water ($\theta \approx 48°$) around Planes 2 and 3 with respect to bulk water indicates that the protein appears to disrupt the ordering of solvation water around these faces, as described above. This effect does not seem to be specific to the non-ice-binding surfaces of AFPs. Hydrophilic residues, such as those found on Planes 2 and 3, are generally found to decrease the population of tetrahedral water molecules in their solvation shell.[40−42] It therefore seems likely that the non-ice-binding surfaces of CfAFP have evolved to be hydrophilic, since such residues perform the required function, without further specificity. This hypothesis is supported by the observation that non-ice-binding residues are not conserved between different isoforms of CfAFP.[44]

If the ordering of water leads to greater ice-binding, it would be expected that the ordered water has some structural similarity to the ice surface involved. Using the aligned trajectory (see Methods), the density of water molecules within a region defined by $-16 \le x \le 16$, $-12 \le y \le 12$, and $0 \le z \le 10$ was determined and is shown in Figure 4. Although the z-dependence of the density is lost due to the difficulty of representing four-dimensional data, clear features can nevertheless be observed. The aligned protein does not quite fall along the x-axis, but is rotated slightly clockwise and lies parallel to the density features. That such a clear grid of features can be observed is quite remarkable. It is known that the ice-binding threonine residues are closely commensurate with the lattice parameters of both the basal and prism planes of ice,[5] and these results demonstrate that this feature is conferred on the adjacent solvation water. The spacings between the density peaks are between 2 and 3 Å along the approximate y-direction and between 4 and 5 Å along the approximate x-direction, providing a reasonable match to both the prism and basal planes of ice. The ice-binding plane therefore not only orders the water molecules, but creates a match with the ice surface to which binding occurs, maximizing the compatibility between the protein and the surface and minmising the entropy loss occurring on binding. Away from the ice-binding region, the density is approximately uniform, as expected for mobile water molecules.

3.2. Water Mobility Is Reduced around the Ice-Binding Face. In addition to considering time-averaged structural properties, the dynamics of water molecules close to the protein are also examined. Recent studies have shown that the diffusional

(44) Doucet, D.; Tyshenko, M. G.; Kuiper, M. J.; Graether, S. P.; Sykes, B. D.; Daugulis, A. J.; Davies, P. L.; Walker, V. K. *Eur. J. Biochem.* **2000**, *267*, 6082–6088.

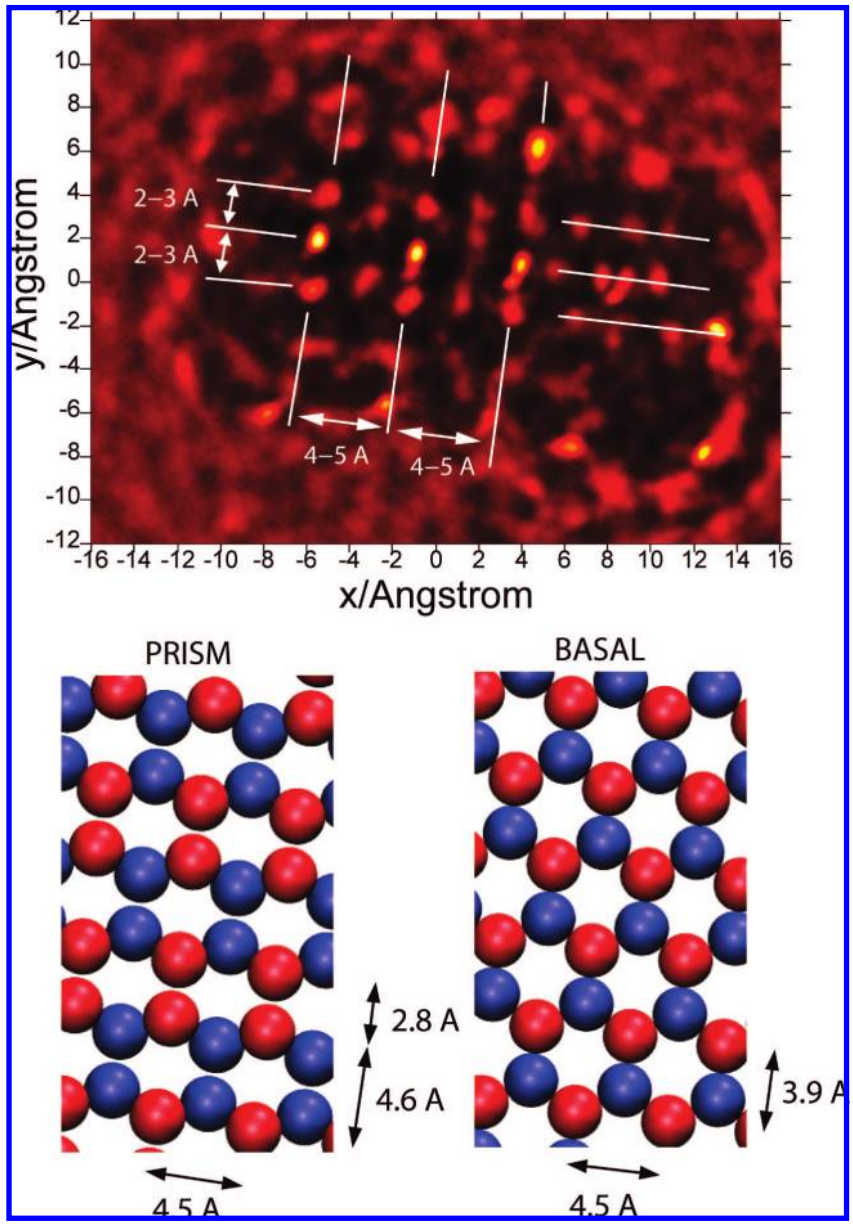

Figure 4. Average water density adjacent to the ice-binding plane of CfAFP at 250 K. The density increases from black to white. The spacings between the regular grid of features are as shown. Comparison is made with the prism and basal planes of ice, for which the upper-most oxygen atoms are colored red, the second plane in blue.

and rotational dynamics of water are slowed significantly in the first few solvation shells of biomolecules.[45−47] Here we examine the mean-square displacement and the reorientational lifetime of the water molecules around the different faces of the protein. The mean-square displacement, $\langle r^2(t)\rangle$, is defined as

$$\langle r^2(t)\rangle = \langle |\vec{r}_i(t) - \vec{r}_i(0)|^2 \rangle \quad (2)$$

and is related to the 3-dimensional diffusion constant, D, through the Einstein relation

$$D = \lim_{\Delta t \to \infty} \frac{\langle |\vec{r}_i(t) - \vec{r}_i(0)|^2 \rangle}{6\Delta t} \quad (3)$$

The reorientational dynamics can be described by the autocorrelation function of the water dipole moment vector, μ

$$C_\mu(t) = \langle \mu(0)\mu(t) \rangle \quad (4)$$

Results are presented in Figure 5. At 300 K, the dynamic properties around each face of the protein are the same. In the first solvation shell, the diffusion constant is smaller than in the bulk and the reorientational lifetime is longer, as would be expected from existing models of biomolecular solvation.[45,48] The properties of the second solvation shell are almost bulklike.

In contrast, at 250 K, clear differences emerge between the protein faces. Both the reorientational and translational dynamics around the ice-binding face (Plane 1) are considerably slowed relative to Planes 2 and 3, indicating that Plane 1 has a strong

(45) Pal, S. K.; Peon, J.; Bagchi, B.; Zewail, A. H. *J. Phys. Chem. B* **2002**, *106*, 12376–12395.
(46) Bhide, S. Y.; Berkowitz, M. L. *J. Chem. Phys.* **2005**, *123*, 224702.
(47) Pal, S.; Maiti, P. K.; Bagchi, B. *J. Chem. Phys.* **2006**, *125*, 234903.
(48) Bhattacharyya, S. M.; Wang, Z.-G.; Zewail, A. H. *J. Phys. Chem. B* **2003**, *107*, 13218–13228.

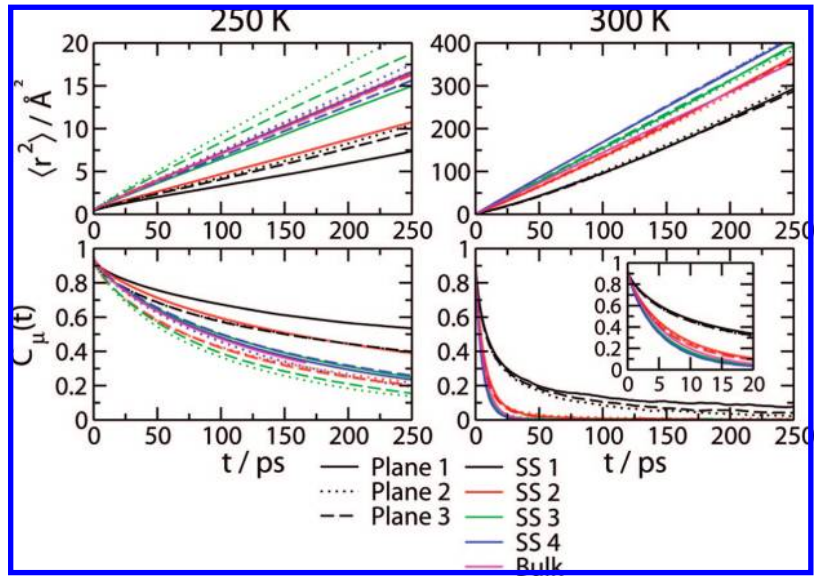

Figure 5. Dynamic properties of solvation water around the different planes of CfAFP at 250 (left) and 300 K (right). Top: Mean-square displacement, $<r^2(t)>$, and bottom: dipole−dipole orientational autocorrelation function, $C_\mu(t)$. The three protein planes are represented with solid (Plane 1), dotted (Plane 2) and dashed lines (Plane 3) and the solvation shells (SS) with black, red, green and blue for SS 1−4, respectively. The corresponding properties for bulk water are shown in magenta. The dynamics are slowed around the ice-binding face (Plane 1) at 250 K, and enhanced around Planes 2 and 3. The short-time behavior of $C_\mu(t)$ at 300 K is shown in the inset.

effect on the adjacent water molecules. Indeed, the dynamical properties of the first solvation shell around Planes 2 and 3 are similar to those of the second solvation shell around Plane 1, suggesting that the first solvation shell around Plane 1 can almost be considered to be a part of the protein. Around Plane 1, the dynamics of the solvation water converge smoothly to the bulk behavior, but different behavior is seen for Planes 2 and 3. The second solvation shell (SS2) around Planes 2 and 3 has bulklike dynamics, with the properties of SS3 exhibiting translational and reorientational dynamics faster than the bulk, before converging to bulk behavior in SS4. This reveals a strong disruption of the water dynamics around the non-ice-binding faces of the protein, where the liquid character of the solvent is enhanced above that of the bulk at the temperature in question. Similar dynamical effects have been observed on hydrophilic surfaces, such as silicon, where the water layers close to the surface exhibit dynamics typical of temperatures 25 degrees higher than the corresponding bulk temperature.[49] That the effect is only observed for a relatively small number of solvation shells is most likely due to the small size of the protein face, compared to bulk materials. The linear behavior of $\langle r^2(t) \rangle$ for all solvation shells at 250 K clearly indicates that the solvent is a supercooled liquid and not a glass, as stated above.

3.3. Hydrogen Bond Lifetimes Are Increased around the Ice-Binding Face. Liquid water is characterized by a network of hydrogen bonds between individual water molecules. This network can be disrupted by the presence of solutes, leading to the formation of structures such as clathrates.[50] The disruption is reflected in the distribution of hydrogen bond strengths and lifetimes, although the two are not necessarily correlated.[29] Here, we define a hydrogen bond according to the geometric criteria of ref 51 corresponding to an oxygen−oxygen distance of less than 3.5 Å and a O−H···O angle of greater than 150°. Two hydrogen bond lifetime correlation functions can then be defined[52] as

$$C_{\mathrm{HB}}(t) = \frac{\langle h(0)h(t) \rangle}{\langle h^2 \rangle} \tag{5}$$

and

$$S_{\mathrm{HB}}(t) = \frac{\langle H(0)H(t) \rangle}{\langle H^2 \rangle} \tag{6}$$

where h is a binary variable equal to 1 if a hydrogen bond is present between two water molecules at time t and angle brackets indicate a time average over all pairs of water molecules. $H(t)$, on the other hand, is equal to 1 if a hydrogen bond exists between two water molecules at time t and has existed continuously since time $t = 0$. $S_{\mathrm{HB}}(t)$ is therefore dependent on the history of the hydrogen bond (and therefore on the time resolution of the trajectory data), whereas $C_{\mathrm{HB}}(t)$ is not.

The results are shown in Figure 6. The overall behavior as a function of solvation shell number is similar to that observed to the reorientational and translational dynamics, illustrating the fact that water dynamics are highly complex and individual processes are closely coupled.[29,53] At 300 K, the hydrogen bond dynamics are slowed in the first solvation shell to the same extent around each of the three faces of the protein. The second solvation shell is only marginally affected by the protein, and bulk behavior is observed for solvation shells 3 and 4. Visual inspection and model function fitting (not shown for clarity) show that the behavior of C_{HB} has two time scales: a short time scale which is strongly dependent on the solvation shell and a longer time scale which is similar for all shells. S_{HB} behaves quite differently, with only the first solvation shell having

(49) Ochshorn, E.; Cantrell, W. *J. Chem. Phys.* **2008**, *128*, 134701.
(50) Nada, H. *J. Phys. Chem. B* **2006**, *110*, 16526–16534.
(51) Luzar, A.; Chandler, D. *Phys. Rev. Lett.* **1996**, *76*, 928–931.
(52) Pal, S.; Bagchi, B.; Balasubramanian, S. *J. Phys. Chem. B* **2005**, *109*, 12879–12890.
(53) Laage, D.; Hynes, J. T. *Science* **2006**, *311*, 832–835.

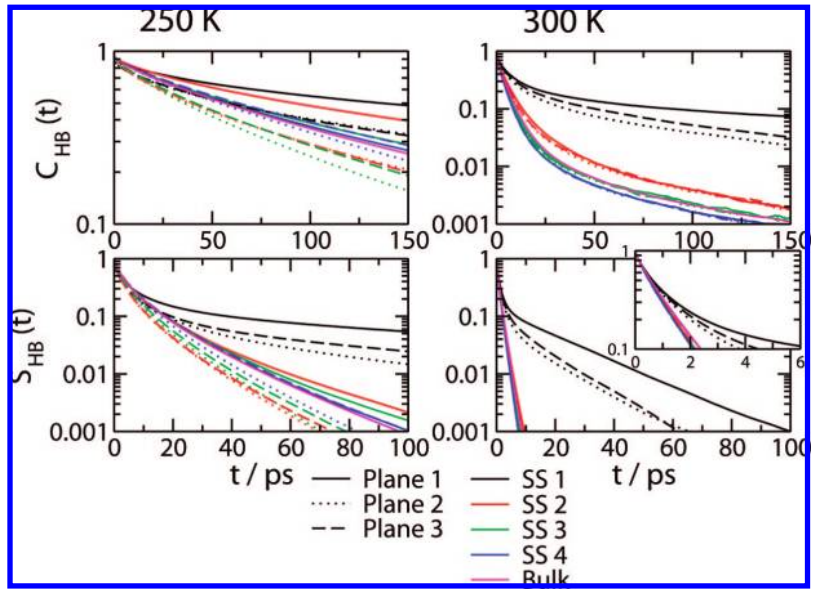

Figure 6. Hydrogen bond lifetime correlation functions $C_{HB}(t)$ (top) and $S_{HB}(t)$ (bottom) for water around the different planes of CfAFP at 250 (left) and 300 K (right). Note the logarithmic scale on the *y*-axis and the different scales for $C_{HB}(t)$ at 250 and 300 K. The three protein planes are represented with solid (Plane 1), dotted (Plane 2), and dashed lines (Plane 3) and the solvation shells (SS) with black, red, green, and blue for SS 1−4, respectively. The corresponding properties for bulk water are shown in magenta. The hydrogen bond lifetime is increased around the ice-binding face (Plane 1) at 250 K, compared to Planes 2 and 3. The short-time behavior for $S_{HB}(t)$ at 300 K is shown in the inset.

biexponential behavior. Within this shell, the water around Plane 1 is slightly slower than the water around Planes 2 and 3. S_{HB} for the more distant solvation shells was found to have a single-exponential decay.

At 250 K, the dynamics becomes more complex. Nevertheless, several key features can be noted which reinforce the observations made above. First, the hydrogen bond dynamics of the water in the first solvation shell around Plane 1 are clearly slower than all other cases. Even the water molecules in solvation shell 2 of Plane 1 are significantly slowed with respect to bulk water, and these have similar properties to the water in shell 1 around Planes 2 and 3, as found for the reorientational and translational dynamics. Around Plane 1, the dynamical properties converge smoothly to the bulk values, as would be expected. However, the convergence of the dynamics around Planes 2 and 3 is not smooth: once again, the hydrogen bond dynamics of shells 2 and 3 are faster than in the bulk, with a shorter lifetime, before converging to the bulk behavior in shell 4. This behavior is observed for both C_{HB} and S_{HB} at 250 K.

4. Discussion and Conclusions

At 250 K, the water structure and dynamics around the ice-binding face (Plane 1) of CfAFP are significantly different to those around the other two faces (Planes 2 and 3). In particular, the water structure is enhanced and the dynamics are slowed. The effect of the protein is found to extend out to the second and third solvation shells. Around Planes 2 and 3, the hydrogen bond dynamics in the second and third solvation shells are faster than in the bulk at the same temperature, consistent with disruption of the water. The translational dynamics are also slightly faster than the bulk. At 300 K, on the other hand, no significant differences are observed between the three protein planes and only the first solvation shell is strongly affected by the protein. There is therefore a delicate balance between protein−water and water−water interactions. On the basis of the present observations, the influence of the ice-binding residues on the solvation water increases as the temperature is reduced from 300 to 250 K, such that water ordering is sufficient for enhanced protein-surface binding at physiologically relevant temperatures (around 273 K). Stronger interactions could increase the size of the preconfigured solvation shell further, with the potential consequence of providing a nucleation site, which would defeat the purpose of the antifreeze protein. Ice-nucleating proteins do exist, but their functional role is quite different to the AFPs.[2] Weaker interactions would not be able to order the solvation shell and would therefore lead to a larger energy barrier for surface binding. Once again, biology has provided a highly tuned tool with a delicate balance of interactions in order to perform the required function as efficiently as possible.

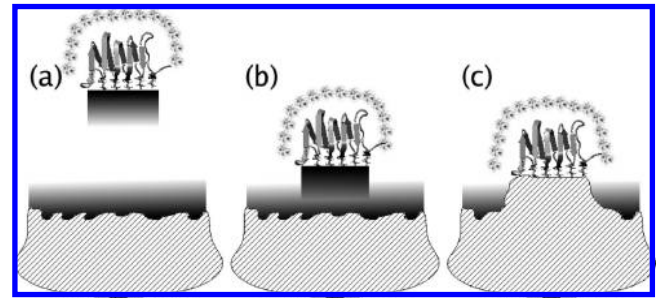

Figure 7. Schematic of the proposed ice-binding mechanism. The shading represents the ordering at the ice−water and protein−water interfaces and the texture represents water disruption. As the protein approaches the ice surface, the ordered regions overlap (b). Localized ice growth then incorporates the ice-binding face of the protein (c). Disruption of the water structure around the rest of the protein protects it from being overgrown.

The present results suggest the following mechanism for the ice-binding process (see Figure 7). When the AFP is in aqueous solution at sufficiently low temperature, the solvation shell around ice-binding face becomes more structured and experiences slowed dynamics. This creates a "pre-ordered" region in which the barrier to ice formation is reduced (Figure 7a). (Note that antifreeze proteins themselves do not nucleate ice: ice-nucleation proteins are typically much larger in order to be able

to stabilize ice particles with sizes approaching the critical radius for ice formation.[54]) When the protein comes into contact with the molecularly rough interfacial region between bulk ice and bulk liquid water (around 10−15 Å thick), the noncrystalline ordered zone at the ice:water interface merges with the AFP preordered zone (Figure 7b). This facilitates a localized growth of ice which incorporates the partially ordered solvation shell. If the growing ice surface is of the correct plane and the orientation of the AFP is favorable, the ice-binding face can then be incorporated into the ice lattice.[14]

A further significant result of the present work is a clear indication that the protein has also evolved in order to avoid being incorporated into the growing ice. It appears to do this by disrupting the water structure around the non-ice-binding faces of the protein. The first layer of solvation water binds strongly to hydrophilic residues as indicated by the large first peak in the density distribution function, $g(r)$. The mobility of these molecules is reduced, and they cannot form strong hydrogen bonds to subsequent layers. This leads to less structuring and faster dynamics in shells 2 and 3 than would be expected at the bulk temperature. On the basis of NMR data, it has previously been proposed that amino acid side chains on the non-ice-binding parts of the surface are more mobile than those on the ice-binding face,[55,56] leading to disruption of the water structure. The present results clearly indicate that disruption of the solvation shells does occur. Comparison with water dynamics at bulk surfaces shows that a hydrophilic surface is sufficient to generate this effect[49] and that no side-chain or surface motion is necessary, although this could enhance the effect further. The present study demonstrates how water molecule dynamics is correlated with the AFP function. Interestingly, disruption of water structure (rather than compatibility with ice surfaces) has recently been proposed to be involved in the function of recrystallization inhibitors, such as antifreeze glycoproteins and their analogues.[57] It is therefore possible that the non-ice-binding residues play a more significant role than previously thought.

These results provide strong evidence to indicate that AFPs are involved in the construction of their own binding site by encouraging the local growth of ice. The results support and significantly extend previous simulation work in which it was suggested that the ice-binding surface of the protein may lead to ordering of the water molecules in the interfacial region between bulk ice and water.[21−23] The present simulations indicate that the solvation shells around the AFP ice-binding surface play an important role in the physiological function of an AFP. The results are consistent with previous modeling studies of solvation water around other AFPs (Type I AFP from winter flounder[24,42] and type III AFP from eel pout),[23,40,41] suggesting that this is a general phenomenon occurring in ice-binding and recognition. An interesting comparison with general receptor−ligand interactions can then be made. If the ordered solvation shell is considered to be an integral part of the protein (ligand), the binding to the ice surface (receptor) can potentially be viewed as an example of an induced-fit binding mechanism.

Once the protein has initially bound to the surface, it is possible that final attachment of the entire ice-binding surface of the protein occurs in a zipper-like fashion, in which the ice-binding surface stabilizes the growing ice surface once initial binding has occurred.[20] The driving force for protein−ice binding could potentially be due to a reduction in interfacial energy. During binding, the ice−water interface and protein−ordered water−bulk water interface merge, with the preordering reducing the entropic cost as much as possible, giving an overall reduction in the free energy of the system. The binding would therefore be irreversible, as observed experimentally. An understanding of the preference of antifreeze proteins for specific ice surfaces (100, $2\bar{1}0$, 111, etc.) and an evaluation of the zipper mechanism could therefore be addressed by considering the properties of AFPs at the appropriate ice−water interface and will require simulations which explicitly include this interfacial region,[21,22] as well as using a suitable water model for these conditions. Such studies may provide an answer to the question of how AFPs compete against 55 M water for efficient and effective surface binding, as well as providing insight into the significant effects that single mutations on the ice-binding surface can have on antifreeze activity.[5]

The detailed analysis of the dynamics in this work reveals the role of the non-ice-binding regions of the protein. Strong interactions between the protein and the first shell of solvation water leads to a disruption of structure and faster dynamics in the second and third shells, providing protection against ice growth which could potentially have engulfed the protein. It remains to be investigated whether the hyperactivity of AFPs such as CfAFP is due to the properties of the ice-binding or non-ice-binding faces. It is clear, however, that both regions play an important role in the biological function of this protein.

The present "pre-ordering-binding" mechanism for initial recognition and subsequent attachment of AFPs to ice may also be generally applicable to processes occurring at disordered surfaces, for example, the transition of amorphous calcium carbonate to crystalline calcite occurring in the presence of macromolecules.[58] This important issue deserves further investigation. Our findings shed new light on the molecular-level processes involved in the recognition and binding of biomolecules to ice and demonstrate once again that "biological water" (as opposed to bulk water) has unique properties and can have potentially important physiological roles.

Acknowledgment. D.R.N. is grateful to the Swiss National Science Foundation (SNF) for the award of an Advanced Research Fellowship.

JA8034027

(54) Zachariassen, K. E.; Kristiansen, E. *Cryobiology* **2000**, *41*, 257–279.
(55) Daley, M. E.; Sykes, B. D. *Protein Sci.* **2003**, *12*, 1323–1331.
(56) Daley, M. E.; Sykes, B. D. *J. Biomol. NMR* **2004**, *29*, 139–150.
(57) Czechura, P.; Tam, R. Y.; Dimitrijevic, E.; Murphy, A. V.; Ben, R. N. *J. Am. Chem. Soc.* **2008**, *130*, 2928–2929.
(58) Raz, S.; Hamilton, P. C.; Wilt, F. H.; Weiner, S.; Addadi, L. *Adv. Funct. Mater.* **2003**, *13*, 480–486.